ANALYSIS OF VOLTAGE MODEL-BASED ROTOR FLUX ESTIMATION FOR CLOSED-LOOP CONTROL METHODS WITHOUT SPEED ENCODER

Cuong Dinh Tran*, Khoa Dang Tran Phan

Faculty of Electrical and Electronics Engineering,

Ton Duc Thang University, Ho Chi Minh City, Viet Nam

*Email: *trandinhcuong@tdtu.edu.vn*

Received: 18 January 2026; Revised: 13 March 2026; Accepted: 16 March 2026

ABSTRACT

Induction motors (IMs) are key components in numerous industrial drive systems due to their simple structure, low cost, and high reliability. However, achieving accurate and robust speed control under varying load conditions remains a significant challenge, particularly for sensorless drive systems. This paper investigates the effectiveness of the Model Reference Adaptive System (MRAS). The speed estimation technique is applied to two commonly used IM control strategies: scalar control using the voltage model (SC-VM) and field-oriented control using the voltage model (FOC-VM). In both approaches, the rotor speed and flux angle are directly estimated from measured stator voltage and current signals, thereby eliminating the need for mechanical speed sensors. Simulation results obtained under various operating conditions demonstrate that the MRAS-based sensorless control strategy provides high estimation accuracy, good dynamic response, and stable system performance, while reducing system cost and simplifying the drive structure. A comparative analysis further indicates that scalar control is well-suited for applications with low cost and simple structural requirements, whereas field-oriented control better meets demands for high dynamic performance and high control accuracy. These findings offer valuable insights for selecting appropriate control strategies in practical induction motor drive applications.

Keywords: Voltage model, Scalar control, Field-oriented control, MRAS.

1. INTRODUCTION

Induction motors (IMs) are widely used in industry due to their simple structure, low cost, and high robustness [1, 2]. However, achieving accurate and stable speed control under load changes and parameter deviations remains a significant technical challenge. Two popular control strategies today are scalar control (SC) and field-oriented control (FOC).

SC methods, especially the V/f strategy, have outstanding advantages in simplicity and low implementation cost. However, SC lacks a feedback mechanism and is susceptible to slippage, leading to poor performance in low-speed regions and when the load varies [3, 4]. SC can be implemented in two primary forms: open-loop control [5, 6] and closed-loop control [7, 8]. In open-loop mode, the voltage and frequency are set according to predefined rules, without feedback from the motor. Therefore, the error is difficult to correct, the efficiency is low, and it does not meet the requirements of precise speed and torque control. In closed-loop control, speed and current sensors provide input signals to the controller, and feedback information is used to adjust the voltage and frequency supplied to the motor.

In contrast, FOC provides a clear separation between flux and torque control, along with fast dynamic response and high accuracy [9-11]. However, the main drawback of typical FOC is its reliance on the mechanical sensor, such as encoders, to determine rotor speed or flux angle [12]. The use of mechanical encoders not only increases the hardware cost but also reduces reliability in harsh industrial environments, where mechanical sensors are prone to failure or performance degradation.

Many studies have compared SC and FOC, confirming FOC's superiority in speed and torque control [13, 14]. Meanwhile, studies in [15, 16] show that SC is still suitable for economic drives. Other studies have focused on torque-speed characteristics, flux-weakening region, current quality, and THD [17-20]. However, most of these works still assume the presence of an encoder, not fully exploiting the potential of sensorless methods.

To solve this problem, sensorless control methods have received much attention in recent years [21, 22]. Model reference adaptive systems (MRAS) have been extensively developed to calculate the rotor flux and its angle in induction motors. MRAS mainly uses two types of models: current models (also called adaptive models) and voltage models (also called reference models) [23-29]. These challenges motivate the development of advanced estimation techniques capable of improving the accuracy and robustness of sensorless induction motor drives under varying load conditions. Table 1 presents the expected performance comparison between these two methods.

Table 1. Theoretical performance comparison between SC and FOC

Criterion	SC [3-8]	FOC [2], [9], [10], [12], [14], [18]
Control complexity	Low, easy to implement	High, requires multiple PIs and coordinate transforms
Computation load	Light	Heavier
Cost	Low (no encoder, simple hardware)	Medium (no encoder but higher computation)
Dynamic response	Improved and open-loop SC, but limited	Superior, fast decoupling of flux and torque
Steady-state accuracy	Better than open-loop SC but sensitive to R_s	High, less affected by parameter errors
Parameter sensitivity	Strongly affected by R_s	Less sensitive due to closed-loop structure
Reliability	Improved (no encoder) but limited at low speed	Improved (no encoder) and maintains high performance
Suitable applications	Low cost, medium performance	High-performance industrial applications

In this study, the method of estimating the rotor flux angle using voltage models (VM) is applied instead of encoders. VM uses stator voltage and current signals, along with machine parameters, to calculate the rotor flux vector, thereby determining the flux position with a simple structure and no additional hardware. In this context, to clarify the potential advantages and limitations of the two improvement methods, this paper constructs a performance comparison matrix for SC and FOC based on the voltage model (SC-VM and FOC-VM). Important criteria commonly used in powertrain system evaluation include complexity, computational volume, cost, dynamic response, accuracy, parameter sensitivity, and reliability.

The remainder of the paper is organized as follows: Section 2 presents the IM mathematical model in the (α, β) frame and an improved MRAS-based speed estimation method; next, the SC-VM and FOC-VM control structures are introduced; then, simulation results are presented; and finally, conclusions are drawn.

2. INDUCTION MOTOR MODELLING

2.1. Mathematical modelling in the (α, β) frame

In the stationary (α, β) frame, the dynamic performance of an induction motor (IM) is characterized by core voltage and flux-linkage equations. These illustrate the interconnections among the stator currents, rotor flux elements, and motor parameters, as shown in (1) - (4).

$$\vec{u}_s = R_s \vec{i}_s + \frac{d\vec{\psi}_s}{dt} \tag{1}$$

$$0 = R_r \vec{i}_r + \frac{d\vec{\psi}_r}{dt} - j\omega_r \vec{\psi}_r \tag{2}$$

$$\vec{\psi}_s = L_s \vec{i}_s + L_m \vec{i}_r \tag{3}$$

$$\vec{\psi}_r = L_m \vec{i}_s + L_r \vec{i}_r \tag{4}$$

By integrating (1) through (4), the expression for the electromagnetic torque is obtained as shown in (5).

$$T_e = \frac{3}{2} p L_m \operatorname{Im}\{\vec{i}_s \vec{\psi}_r\} \tag{5}$$

Where: $\vec{i}_s, \vec{i}_r$: stator and rotor current vectors; $\vec{\psi}_s, \vec{\psi}_r$: stator and rotor flux-linkage vectors; R_s, R_r : stator and rotor resistances; L_s, L_r, L_m : stator, rotor, and magnetizing inductances; ω_r : rotor electrical angular speed; p : number of pole pairs; T_e : electromagnetic torque.

This mathematical model forms the theoretical basis for both scalar control (SC) and field-oriented control (FOC). While SC primarily relies on the voltage frequency ratio to regulate flux, FOC exploits full current or flux dynamics to decouple torque and flux control.

2.2. MRAS observer design based on voltage model

The improved Model Reference Adaptive System (MRAS) consists of two distinct models: the reference model, known as the voltage model (VM), employs stator voltage and current to determine components of the rotor flux vector, while the adaptive model, referred to as the current model (CM), utilizes stator current along with the estimated rotor speed to calculate rotor flux components. To achieve this, the measured stator voltages and currents were converted from the three-phase (*a, b, c*) reference frame to the stationary (*α, β*) frame using the Clarke transform [22].

The VM-based MRAS is used to estimate speed in sensorless mode. The principle is to compare the rotor flux computed by VM with that from CM. The error between the two models is fed to an adaptive PI controller, which updates the estimated rotor speed. Figure 1 shows the structure of the rotor flux-based speed observer in the improved MRAS [30].

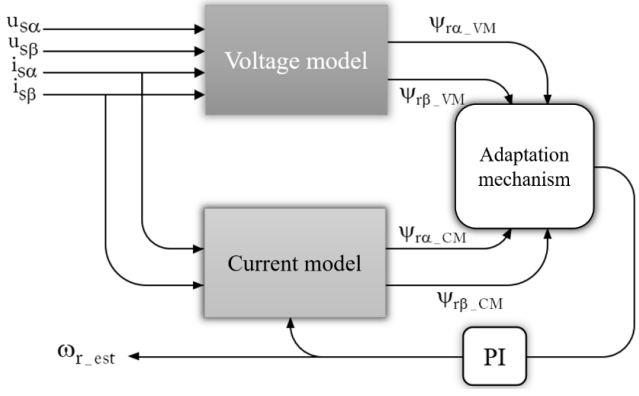

Figure 1. MRAS model for speed estimation based on the VM

In the stationary (*α, β*) frame, the rotor flux components of the VM are expressed via the IM voltage equations, as in (6) and (7).

$$\psi_{r\alpha\_VM} = \frac{L_r}{L_m}\left[\int (u_{s\alpha} - R_s i_{s\alpha})dt - \frac{L_s L_r - L_m^2}{L_r} i_{s\alpha}\right] \tag{6}$$

$$\psi_{r\beta\_VM} = \frac{L_r}{L_m}\left[\int (u_{s\beta} - R_s i_{s\beta})dt - \frac{L_s L_r - L_m^2}{L_r} i_{s\beta}\right] \tag{7}$$

The rotor flux in the CM is computed from the estimated speed and stator current dynamics, as in (8) and (9).

$$\psi_{r\alpha\_CM} = \int \left(\frac{L_m}{T_r} i_{s\alpha} - \frac{1}{T_r}\psi_{r\alpha\_CM} - \omega_{r\_est}\psi_{r\beta\_CM}\right) dt \tag{8}$$

$$\psi_{r\beta\_CM} = \int \left(\frac{L_m}{T_r} i_{s\beta} - \frac{1}{T_r} \psi_{r\beta\_CM} + \omega_{r\_est} \psi_{r\alpha\_CM} \right) dt \tag{9}$$

The estimated rotor speed is obtained via an adaptive PI mechanism, as in (10) and (11):

$$f(e) = \psi_{r\alpha\_CM} \psi_{r\beta\_VM} - \psi_{r\alpha\_VM} \psi_{r\beta\_CM} \tag{10}$$

$$\omega_{r\_est} = K_p f(e) + K_i \int_0^t f(e) dt \tag{11}$$

Here $T_r = L_r / R_r$ denotes the rotor time constant, $f(e)$ represents the flux error function used as the adaptation signal, ω_{r_est} is the estimated rotor speed, K_p, K_i are the proportional and integral gains of the adaptive PI controller.

Based on the rotor flux components $\psi_{r\alpha\_VM}$ and $\psi_{r\beta\_VM}$ in (8) and (9), the rotor flux angle (γ_r) is computed by (12).

$$\gamma_r = \arctan\left(\frac{\psi_{r\beta\_VM}}{\psi_{r\alpha\_VM}} \right) \tag{12}$$

This estimated angle is then applied to both SC and FOC structures.

2.3. Stability analysis of the MRAS observer's frame

The stability of the MRAS-based speed estimator is theoretically justified using a Lyapunov-based analysis of the adaptive observer [31], [32]. The MRAS scheme employs a voltage model (VM) as the reference model and a current model (CM) as the adaptive model. The difference between the rotor flux vectors from these two models serves as the adaptation signal for rotor speed estimation.

2.3.1. State error model

In the stator stationary reference frame (*α, β*), the derivative equation of the rotor flux estimation error between the reference model (VM) and the adaptive model (CM) can be expressed as follows:

$$\dot{e} = \mathbf{A}e - \Delta\omega_r \mathbf{J} \psi_{r\_CM} \tag{13}$$

Where, $\mathbf{A} = -\frac{1}{T_r}\mathbf{I} + \omega_r \mathbf{J}$ is the system matrix, $\mathbf{J} = \begin{bmatrix} 0 & -1 \\ 1 & 0 \end{bmatrix}$ is the rotation matrix, $\mathbf{I} = \begin{bmatrix} 1 & 0 \\ 0 & 1 \end{bmatrix}$ denotes the identity matrix, and $\Delta\omega_r = \omega_r - \omega_{r\_est}$ is the estimated speed error.

2.3.2. Lyapunov adaptive law

To investigate the system stability, a scalar Lyapunov candidate function *V*, which is globally positive definite, is proposed based on the total energy of the rotor flux error and the speed estimation error:

$$V = \frac{1}{2} e^T e + \frac{1}{2\lambda} \Delta\omega_r^2 \tag{14}$$

With λ is a positive constant representing the adaptation gain.

Taking the first derivative of *V* with respect to time, and assuming that the mechanical time constant of the drive system is sufficiently large so that $\dot{\omega}_r \approx 0$, the following expression is obtained:

$$\dot{V} = e^T \dot{e} + \frac{1}{\lambda} \Delta\omega_r \Delta\dot{\omega}_r \tag{15}$$

By substituting (13) into (15), the following expression is obtained:

$$\dot{V} = e^T \left(-\frac{1}{T_r}\mathbf{I} + \omega_r \mathbf{J} \right) e - e^T \mathbf{J} \psi_{r\_CM} \Delta\omega_r + \frac{1}{\lambda} \Delta\omega_r \dot{\omega}_{r\_est} \tag{16}$$

Due to the orthogonal property of the skew-symmetric matrix, the term $e^T \mathbf{J} e = 0$. The equation is reduced to:

$$\dot{V} = -\frac{1}{T_r} \| e \|^2 + \Delta\omega_r \left[\frac{1}{\lambda} \dot{\omega}_{r\_est} - e^T \mathbf{J} \psi_{r\_CM} \right] \tag{17}$$

Expanding the inner product $e^T \mathbf{J} \psi_{r\_CM}$, the speed update law in a pure integral form is obtained:

$$\omega_{r\_est} = \lambda \int \left(\psi_{r\alpha\_CM} \psi_{r\beta\_VM} - \psi_{r\alpha\_VM} \psi_{r\beta\_CM} \right) dt \tag{18}$$

With the proposed control law, the derivative of the Lyapunov function becomes negative semi-definite:

$$\dot{V} = -\frac{1}{T_r} \| e \|^2 \leq 0 \tag{19}$$

Since V is positive definitevà $\dot{V}$ is negative semi-definite, the system is stable in the Lyapunov sense.

2.4. Quantitative performance evaluation

To objectively compare the dynamic behavior of the control strategies, a quantitative performance metric is required. This work uses the Integral of Time-weighted Absolute Error (ITAE) as the evaluation criterion [33].

For the IM drive system, the ITAE is defined from the speed-tracking error between the reference and actual mechanical speeds and is computed over a fixed observation interval T = 6 s as:

$$ITAE = \int_0^T t \, | (\omega_m - \omega_m^*) | \, dt \tag{20}$$

Where ω_m denotes the measured mechanical angular speed of the induction motor, and ω_m^* represents the reference speed command.

3. CONTROL STRATEGIES IN INDUCTION MOTOR DRIVES

3.1. Improved scalar control using the voltage model

Scalar control (SC), also known as the *V/f* strategy, is widely used due to its simplicity and minimal need for controller parameter tuning. However, its accuracy in speed regulation is limited. In conventional open-loop SC, the basic principle is to adjust the stator voltage amplitude and supply frequency in proportion to the desired motor speed. The speed reference is first converted to the control frequency, which is then used to compute the stator voltage amplitude via (21).

$$V_m = \frac{V_{m\_\text{rated}}}{f_{\text{rated}}} f \tag{21}$$

Where: V_m denotes the control voltage, V_{m_rated} represents the rated control voltage, f is the control frequency, f_{rated} denotes the rated control frequency.

From V_m and f, three-phase reference voltages in the (*a, b, c*) frame are generated. These signals are then modulated using sinusoidal PWM (SPWM) to produce inverter switching pulses supplying the IM.

Although open-loop SC is easy to implement, its performance is limited by poor dynamics and low robustness against load variations. To improve accuracy, a closed-loop SC has been developed, yielding better results than an open-loop SC.

An improved SC strategy is proposed by integrating the VM-based rotor flux angle observer (SC-VM) with slip compensation. The control diagram of the proposed SC-VM is shown in Figure 2. In this structure, the rotor flux angle γ_r from (12) is used to compute the slip frequency. This slip information is fed back to correct the commanded synchronous frequency, thereby improving speed regulation and transient behavior. The synchronous speed of the rotor flux ω_s is determined by differentiating γ_r and the slip frequency ω_{sl} is defined as the difference between ω_s and ω_{r_est}, as in (22) and (23).

$$\omega_s = \frac{d\gamma_r}{dt} \tag{22}$$

$$\omega_{sl} = \frac{1}{p}\left(\omega_s - \omega_{r\_est}\right) \tag{23}$$

Where ω_s denotes the synchronous angular speed, ω_{sl} represents the slip angular speed.

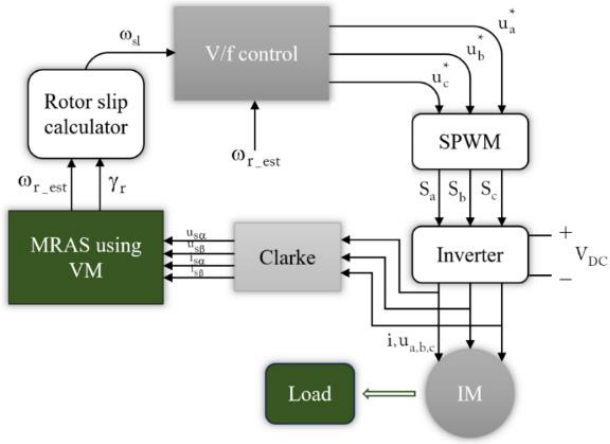

Figure 2. Block diagram of the drive using the improved scalar control (SC-VM)

By compensating for a slip in the speed command, the improved closed-loop SC using VM-based flux-angle estimation achieves higher accuracy, faster response, and better robustness.

3.2. Improved field-oriented control using the voltage model

Field-oriented control (FOC) is a closed-loop vector-control strategy widely used in high-performance IM drives. The principle is analogous to a separately excited DC motor, where flux and torque can be controlled independently. In this method, the stator current is represented as a space vector and decomposed into two orthogonal components in a rotating frame aligned with the rotor flux: i_{sx} regulates flux and i_{sy} regulates electromagnetic torque.

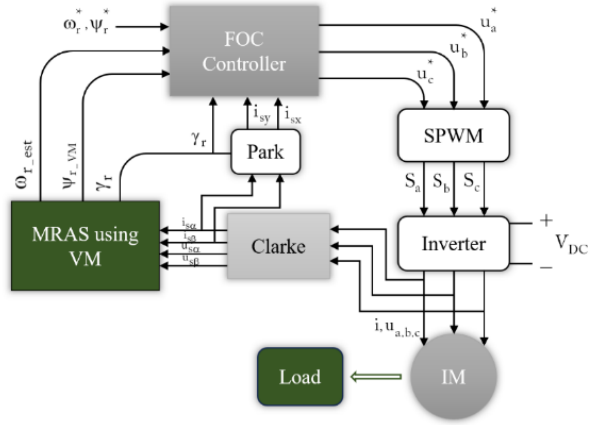

Figure 3. Block diagram of the drive using the improved field-oriented control (FOC-VM)

In practice, measured stator currents and rotor speed from sensors are combined with the motor model to synthesize voltage references. First, the three-phase currents were transformed to the (α, β) frame using the Clarke and the Park transform, which project these components into the rotating (x, y) frame aligned with the rotor flux angle γ_r [27].

The errors between reference quantities (flux, speed) and measured or estimated values are processed by PI controllers. The commands i_{sx}^* and i_{sy}^* are then inverse-transformed to voltage references, which feed the PWM to generate inverter gating signals.

In FOC, accurate knowledge of the rotor flux angle γ_r and rotor speed ω_r is crucial for flux-torque decoupling. Traditional approaches rely on a mechanical encoder to obtain these quantities. However, mechanical sensors may reduce reliability in industrial environments and limit compact drive applications.

To overcome this, we employ FOC using the voltage model (FOC-VM), which directly estimates γ_r and ω_{r_est}. The overall block diagram of the improved FOC with VM is shown in Figure 3. In this structure, VM provides the rotor flux ψ_{r_VM} and rotor flux angle γ_r for the Park transform. As a result, the system achieves precise control with fast dynamics.

4. RESULTS

The rated data and equivalent-circuit parameters of the three-phase IM used in simulations are given in Table 2.

Table 2. IM parameters used in simulation

Parameter	Value
Rated power (P)	2200 W
Rated voltage (V)	380 V
Frequency (f)	50 Hz
Stator/rotor resistance (R_s/ R_r)	3.179/ 2.118 Ω
Stator/rotor/magnetizing inductance (L_s/ L_r/ L_m)	0.209/0.209/0.192 H
Pole pairs (p)	2

In SC-VM, slip compensation is implemented by using the estimated speed from the improved MRAS to correct the supply frequency. After the motor reaches steady state, the compensator is activated with an initial delay (0.7 s) and periodic updates (1.0 s). When load or speed changes occur, the algorithm recalculates slip and adjusts the compensation value, thereby limiting oscillations, reducing overshoot, and making the actual speed closely follow the reference.

Several simulation scenarios were conducted to evaluate and compare the control performance of SC-VM and FOC-VM, including: (i) speed step response, (ii) load step disturbance, and (iii) low-speed operation.

Case 1: Speed step response

In this scenario, the reference speed changes from 355 rpm to 710 rpm at t = 2.0 s under a load of T_L = 5 N·m. The comparative responses of SC-VM and FOC-VM are shown in Figure 4.

With SC-VM, the rotor speed followed the command. Still, the control quality is limited (Figure 4a). The speed error e_ω exhibits a large transient magnitude, with overshoot of 0.8575 and ITAE of 29.29 (Figure 4b). The stator currents (Figure 4c) vary significantly at the speed-change instant. The electromagnetic torque T_e (Figure 4d) showed large oscillations during the transient and takes a long time to settle.

In contrast, with FOC-VM, the rotor speed closely tracked the reference with tiny error (Figure 4e). The speed error e_ω exhibits only 0.03309 overshoot and an ITAE of 2.217 (Figure 4f), indicating a faster, more stable response. The stator currents (Figure 4g) remain symmetric and sinusoidal with a lower magnitude than SC-VM. The electromagnetic torque T_e (Figure 4h) showed a short transient pulse that quickly vanishes, returning to balance with T_L.

The results in Case 1 indicate that FOC-VM outperformed SC-VM in accuracy (overshoot, ITAE) while maintaining smoother, more stable torque during acceleration.

Case 2: Load step disturbance

In this case, the system is subjected to a mechanical load step of T_L = 3 Nm at t = 2.5 s, while the reference speed is kept constant at 710 rpm. The comparative responses of SC-VM and FOC-VM are shown in Figure 5.

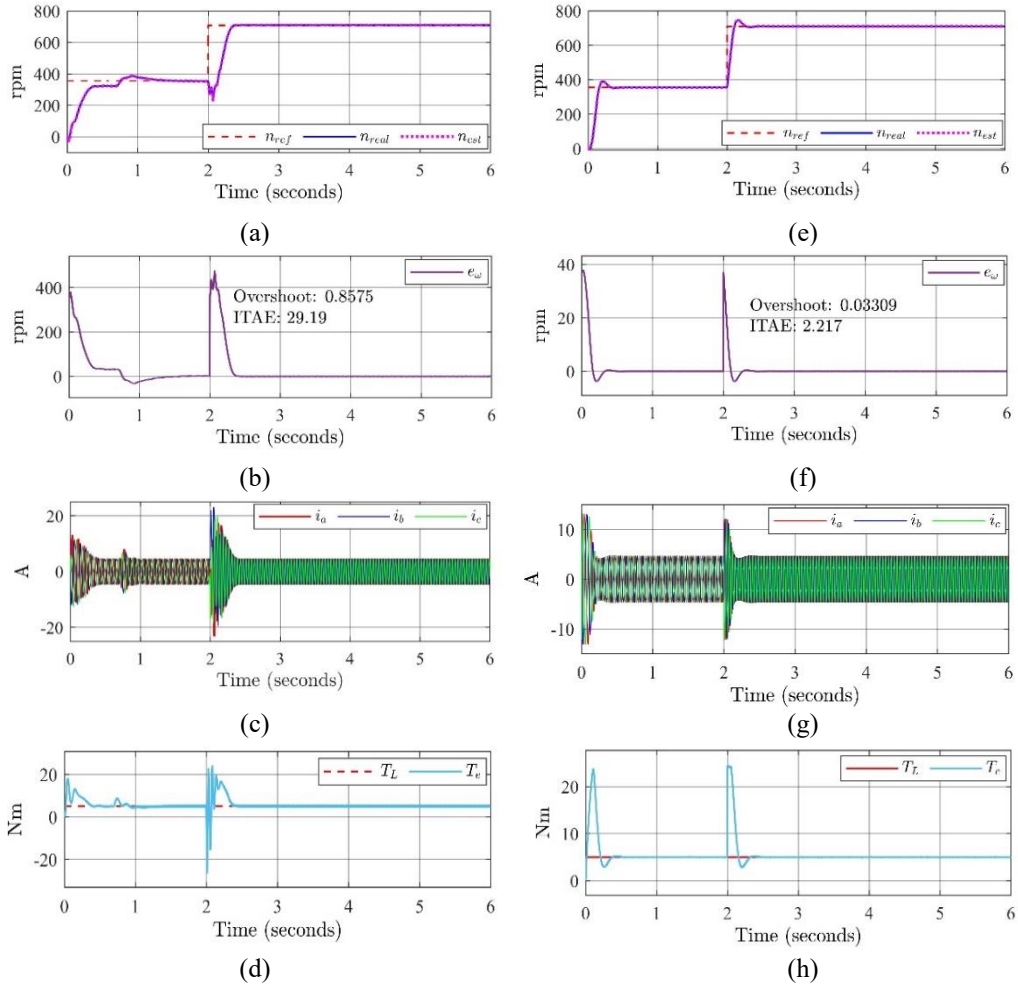

Figure 4. Comparison between SC-VM and FOC-VM in Case 1 (speed step from 355 to 710 rpm at t=2.0 s with T_L=5 Nm): (a, e) Rotor speed vs reference; (b, f) Speed error; (c, g) Stator currents; (d, h) Load and electromagnetic torques.

With SC-VM, the rotor speed tracked the reference but exhibited significant deviation under load disturbance (Figure 5a). The speed error e_ω oscillated vigorously, with an overshoot of -0.3155 and an ITAE of 19.00 (Figure 5b), indicating reduced control quality during the impact. The stator current (Figure 5c) varied considerably at the load-change instant, while the electromagnetic torque T_e (Figure 5d) showed large oscillations and a long settling time.

Meanwhile, with FOC-VM, the rotor speed remains close to the command with only a minor error (Figure 5e). The speed error e_ω has an overshoot of just 0.0332 and an ITAE of 1.176 (Figure 5f), demonstrating markedly better disturbance rejection. The stator currents (Figure 5g) increase their amplitude to compensate for the load, yet remain symmetric and sinusoidal. The electromagnetic torque T_e (Figure 5h) produces only a brief compensation pulse before quickly rebalancing with T_L. The results in Case 2 confirm that FOC-VM achieves superior speed stability under load disturbances, while maintaining good current quality and a smoother torque response than SC-VM.

Case 3: Low-speed operation

In the low-speed scenario with ω_{ref} = 50 rpm and T_L = 1 Nm, the comparison in Figure 6 highlights the performance differences between the two methods.

With SC-VM, the rotor speed failed to maintain the setpoint, showing large oscillations and a prolonged delay (Figure 6a). The speed error eω oscillated severely around the operating point, yielding poor indices: overshoot of -2.394 and ITAE of 52.97 (Figure 6b). The three-phase currents (Figure 6c) are heavily distorted and uneven over time. The electromagnetic torque T_e (Figure 6d) exhibits high

ripple and fails to stabilize at the balance value with T_L. These behaviors clearly demonstrate that SC-VM performs poorly at very low speeds.

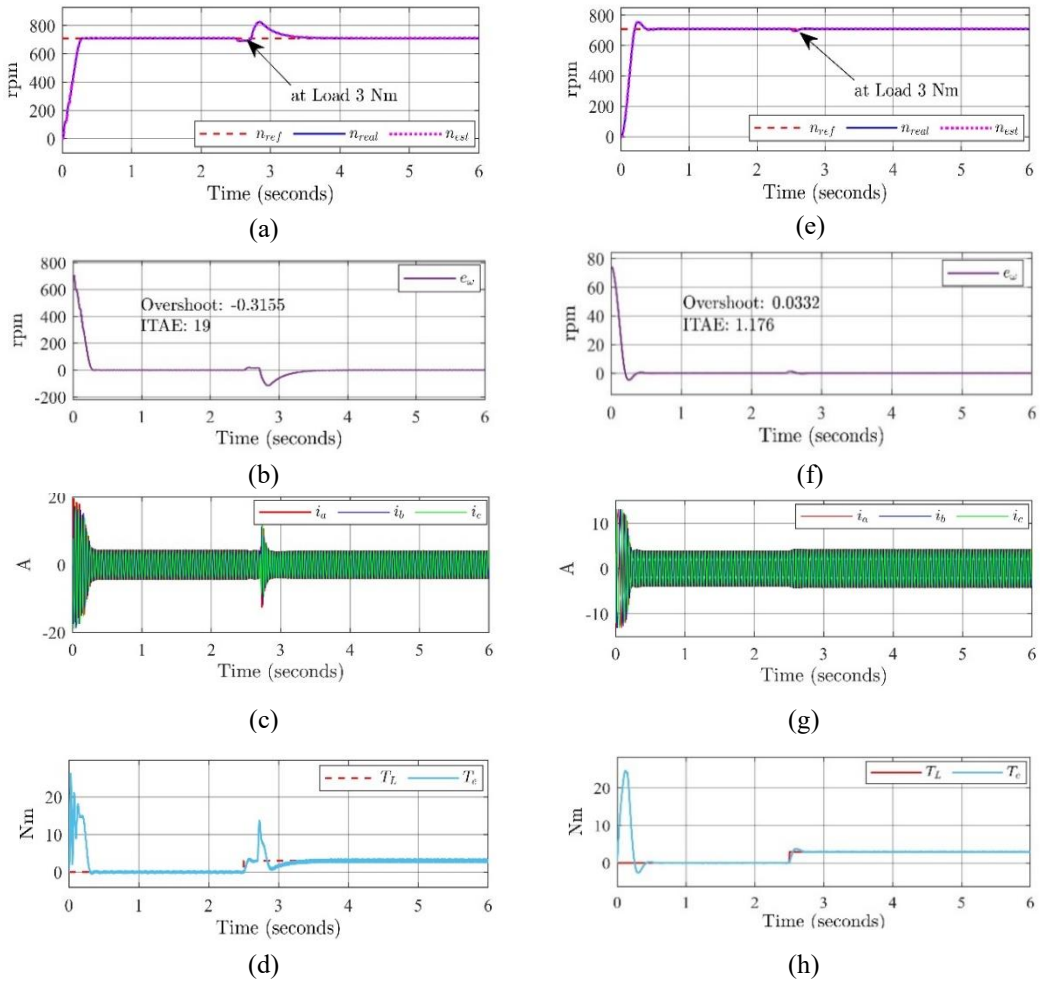

Figure 5. Comparison between SC-VM and FOC-VM in Case 2 (load step at t = 2.5 s, constant reference speed): (a, e) Rotor speed vs reference; (b, f) Speed error; (c, g) Stator currents; (d, h) Load and electromagnetic torques.

In contrast, with FOC-VM, the controller maintains accurate speed tracking (Figure 6e). The speed error e_ω is very small, with overshoot of 0.00919 and ITAE of 0.082 (Figure 6f). The stator currents remain symmetric and sinusoidal (Figure 6g). The electromagnetic torque T_e (Figure 6h) balances with T_L quickly and with minimal ripple.

At very low speeds, SC-VM exhibits severe limitations in speed tracking and torque stability, whereas FOC-VM delivers precise, robust performance.

Table 3. IM parameters used in simulation

Case	SC-VM		FOC-VM	
	Overshoot (%)	ITAE	Overshoot (%)	ITAE
1	0.8575	29.29	0.03309	2.217
2	-0.3155	19.00	0.03320	1.176
3	-2.394	52.97	0.00919	0.082

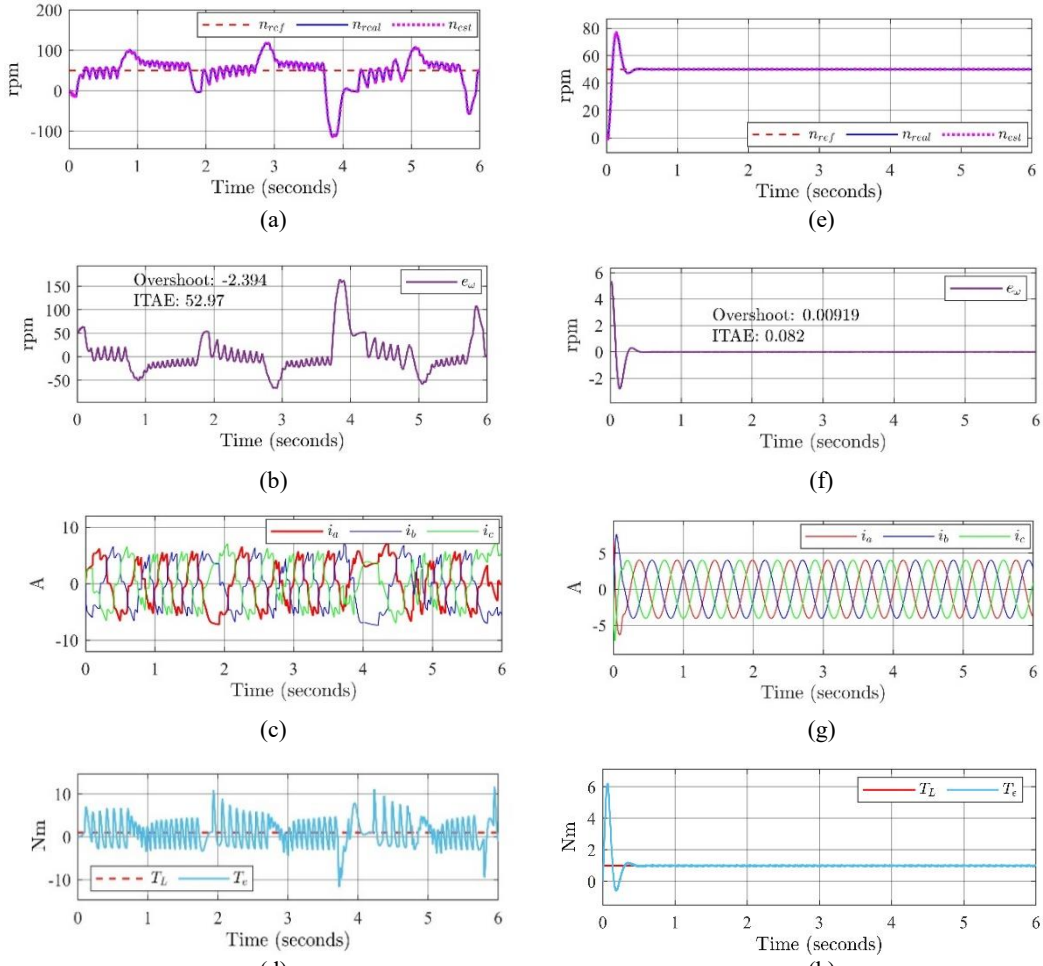

Figure 6. Comparison between SC-VM and FOC-VM in Case 3 (low-speed operation at 50 rpm with T_L=1 Nm): (a, e) Rotor speed vs reference; (b, f) Speed error; (c, g) Stator currents; (d, h) Load and electromagnetic torques.

5. CONCLUSION

The simulation results clearly demonstrate performance differences between SC-VM and FOC-VM in three test scenarios. Specifically, SC-VM with slip compensation partially improves speed tracking, yet still exhibits notable limitations: high overshoot and ITAE in the speed step response, large oscillations under load disturbance, and severe degradation at low speed. Conversely, FOC-VM maintains stable control quality in all cases, with significantly lower overshoot and ITAE, smoother torque, and stable sinusoidal current.

These results confirm the advantage of vector control when combined with VM-based rotor flux angle estimation, especially under complex operating conditions. This indicates that FOC-VM is a more suitable solution for applications requiring accuracy, fast dynamic response, and high current quality. Meanwhile, SC-VM can be considered for simple systems, but its performance is markedly limited at very low speeds or under varying loads. In addition, VM-based sensorless schemes are sensitive to parameter variations, especially stator resistance at low speed. This sensitivity may degrade the accuracy of flux estimation, particularly in SC-VM, and should be considered in practical implementations.

Acknowledgement

This research is funded by Ton Duc Thang University.

REFERENCES

[1] N. G. Ozcelik, U. E. Dogru, M. Imeryuz, and L. T. Ergene, "Synchronous reluctance motor vs. induction motor at low-power industrial applications: Design and comparison," *Energies*, vol. 12, no. 11, Art. 2190, 2019, doi: https://doi.org/10.3390/en12112190.

[2] B. K. Bose, *Power Electronics and Motor Drives: Advances and Trends*. Oxford, U.K.: Elsevier, 2006, doi: https://doi.org/10.1016/C2019-0-02032-8.

[3] H. M. D. Habbi, H. J. Ajeel, and I. I. Ali, "Speed control of induction motor using PI and V/F scalar vector controllers," *International Journal of Computer Applications*, vol. 151, no. 7, pp. 36-43, 2016, doi: https://doi.org/10.5120/ijca2016911831.

[4] M. A. Khettat, K. Hamiche, R. Morvany, C. Annoepel, and A. M. Omara, "Low-cost sensorless scalar control of a brushless motor for automotive fan system application," in *Proc. 23rd Int. Middle East Power Systems Conf. (MEPCON)*, Cairo, Egypt, 2022, pp. 1-6, doi: https://doi.org/10.1109/MEPCON55441.2022.10021740.

[5] J. Jimenez-Gonzalez, J. M. Delgado-Quintero, C. A. Perez-Gomez, I. Lopez-Garcia, V. M. Jimenez-Mondragon, and E. Campero-Littlewood, "Scalar control of squirrel cage induction motors-Fundamentals and scope," in *Proc. IEEE Int. Autumn Meeting on Power, Electronics and Computing (ROPEC)*, Ixtapa, Mexico, 2019, pp. 1-6, doi: https://doi.org/10.1109/ROPEC48299.2019.9057129.

[6] O. Otkun, "Scalar speed control of induction motors with difference frequency," *Journal of Polytechnic*, vol. 23, no. 2, pp. 267-276, 2020, doi: https://doi.org/10.2339/politeknik.474043.

[7] J. M. Pena and E. V. Diaz, "Implementation of V/f scalar control for speed regulation of a three-phase induction motor," in *Proc. IEEE ANDESCON*, Bogota, Colombia, 2017, doi: https://doi.org/10.1109/ANDESCON.2016.7836196.

[8] I. Boldea, A. Moldovan and L. Tutelea, "Scalar V/f and I-f control of AC motor drives: An overview," *2015 Intl Aegean Conference on Electrical Machines & Power Electronics (ACEMP), 2015 Intl Conference on Optimization of Electrical & Electronic Equipment (OPTIM) & 2015 Intl Symposium on Advanced Electromechanical Motion Systems (ELECTROMOTION)*, Side, Turkey, 2015, pp. 8-17, doi: https://doi.org/10.1109/OPTIM.2015.7426739.

[9] S. Kasula, B. Shrestha, K. Katwal, and R. Dahal, "Implementation of indirect field oriented control using space vector pulse width modulation for the control of induction motor," *International Journal on Engineering Technology*, vol. 1, no. 1, pp. 139-152, 2023, doi: https://doi.org/10.3126/injet.v1i1.60936.

[10] M. Gayathri, S. Himavathi, and R. Sankaran, "Performance enhancement of vector controlled drive with rotor flux based MRAS rotor resistance estimator," in *Proc. Int. Conf. Computer Communication and Informatics (ICCCI)*, Coimbatore, India, 2012, pp. 1–6, doi: https://doi.org/10.1109/ICCCI.2012.6158901.

[11] V. S. Malyar, O. Y. Hamola, V. S. Maday, and I. I. Vasylchyshyn, "Mathematical modelling of starting modes of induction motors with squirrel-cage rotor," *Electrical Engineering and Electromechanics*, no. 2, pp. 9-15, 2021, doi: https://doi.org/10.20998/2074-272X.2021.2.02.

[12] H. Chaabane, D. E. Khodja, S. Chakroune, and D. Hadji, "Model reference adaptive backstepping control of double star induction machine with extended Kalman sensorless control," *Electrical Engineering and Electromechanics*, no. 4, pp. 3-11, 2022, doi: https://doi.org/10.20998/2074-272X.2022.4.01.

[13] L. K. Jisha and A. A. Powly Thomas, "A comparative study on scalar and vector control of induction motor drives," in *Proc. Int. Conf. Circuits, Controls and Communications (CCUBE)*, Bengaluru, India, 2013, pp. 1-5, doi: https://doi.org/10.1109/CCUBE.2013.6718554.

[14] M. A. Awdaa, A. A. Obed, and S. J. Yaqoob, "A comparative study between V/F and IFOC control for three-phase induction motor drives," *IOP Conference Series: Materials Science and Engineering*, vol. 1105, 2021, doi: https://doi.org/10.1088/1757-899X/1105/1/012006.

[15] M. A. Martinez-Hernandez, J. m. Gutierrez-Villalobos, S. m. Malagon-Soldara, F. Mendoza-Mondragon and J. Rodriguez-Resendiz, "A speed performance comparative of field oriented control and scalar control for induction motors," *2016 IEEE Conference on Mechatronics,*

Adaptive and Intelligent Systems (MAIS), Hermosillo, Mexico, 2016, pp. 1-7, doi: https://doi.org/10.1109/MAIS.2016.7761902.

[16] G. O. Garcia, R. M. Stephan and E. H. Watanabe, "Comparing the indirect field-oriented-control with a scalar method," *Proceedings IECON '91: 1991 International Conference on Industrial Electronics, Control and Instrumentation*, Kobe, Japan, 1991, pp. 475-480 vol.1, doi: https://doi.org/10.1109/IECON.1991.239339.

[17] G. Kohlrusz and D. Fodor, "Comparison of scalar and vector control strategies of induction motors," *Hungarian Journal of Industry and Chemistry*, vol. 39, no. 2, pp. 265-270, 2011, doi: https://doi.org/10.1515/422.

[18] H. M. Soliman, "Studying the steady state performance characteristics of induction motor with field oriented control comparing to scalar control," *European Journal of Engineering and Technology Research*, vol. 1, no. 2, 2016, doi: https://doi.org/10.24018/ejeng.2016.1.2.115.

[19] M. Bierhoff and J. Büsch, "Novel Scalar versus Field Oriented Speed Control of Induction Machine Drives," *2020 International Symposium on Power Electronics, Electrical Drives, Automation and Motion (SPEEDAM)*, Sorrento, Italy, 2020, pp. 207-212, doi: https://doi.org/10.1109/SPEEDAM48782.2020.9161939.

[20] N. S. Owen, "Investigation and comparison of speed control of an induction motor by V/F control and vector control using MATLAB Simulink," M.S. thesis, Kigali, Rwanda, 2020.

[21] C. D. Tran, P. Brandstetter, M. H. C. Nguyen, S. D. Ho, P. N. Pham, and B. H. Dinh, "An improved current-sensorless method for induction motor drives applying hysteresis current controller," *Indonesian Journal of Electrical Engineering and Informatics*, vol. 9, no. 1, pp. 130-140, 2021, doi: https://doi.org/10.52549/ijeei.v9i1.1619.

[22] C. D. Tran, M. Kuchar, V. Sotola, and P. D. Nguyen, "Fault-tolerant control based on current space vectors against total sensor failures," *Sensors*, vol. 24, no. 11, Art. 3558, 2024, doi: https://doi.org/10.3390/s24113558.

[23] C. Chakraborty and V. Verma, "Speed and current sensor fault detection and isolation technique for induction motor drive using axes transformation," *IEEE Transactions on Industrial Electronics*, vol. 62, pp. 1943-1954, 2014, doi: https://doi.org/10.1109/TIE.2014.2345337.

[24] M. Manohar and S. Das, "Current sensor fault-tolerant control for direct torque control of induction motor drive using flux-linkage observer," *IEEE Transactions on Industrial Informatics*, vol. 13, no. 6, pp. 2824-2833, 2017, doi: https://doi.org/10.1109/TII.2017.2714675.

[25] A. Gholipour, M. Ghanbari, E. Alibeiki, and M. Jannati, "Speed sensorless fault-tolerant control of induction motor drives against current sensor fault," *Electrical Engineering*, vol. 103, no. 3, pp. 1493-1513, 2021, doi: https://doi.org/10.1007/s00202-020-01179-0.

[26] C. D. Tran and N. M. Truong, "Sensorless control for induction motor drive applying CB-MRAS integrating stator resistance estimation," *International Review on Modelling and Simulations (IREMOS)*, vol. 17, no. 4, pp. 215-221, 2024, doi: https://doi.org/10.15866/iremos.v17i4.24107.

[27] F. R. Salmasi, "A self-healing induction motor drive with model free sensor tampering and sensor fault detection, isolation, and compensation," *IEEE Transactions on Industrial Electronics*, vol. 64, no. 8, pp. 6105-6115, 2017, doi: https://doi.org/10.1109/TIE.2017.2682035.

[28] A. Omari, B. I. Khalil, A. Hazzab, B. Bouchiba, and F. Benmohamed, "Real-time implementation of MRAS rotor time constant estimation for induction motor vector control based on a new adaptation signal," *COMPEL: The International Journal for Computation and Mathematics in Electrical and Electronic Engineering*, vol. 38, no. 1, pp. 287-303, 2019, doi: https://doi.org/10.1108/COMPEL-03-2018-0133.

[29] C. D. Tran, M. Kuchar, and P. D. Nguyen, "Improved rotor flux estimation for field-oriented control in induction motor drives," *Technical Electrodynamics*, no. 6, 2025, doi: https://doi.org/10.15407/techned2025.06.052.

[30] T. Xu, Z. Yang, X. Sun, and J. Jia, "Speed sensorless control of a bearingless induction motor based on fuzzy PI fractional MRAS scheme," *International Journal of Green Energy*, vol. 19, no. 4, pp. 389-398, 2022, doi: https://doi.org/10.1080/15435075.2021.1946816.

[31] O. Gulbudak, M. Gokdag, and H. Komurcugil, "Model predictive control strategy for induction motor drive using Lyapunov stability objective," *IEEE Transactions on Industrial Electronics*, vol. 69, no. 12, pp. 12119-12128, 2022, doi: https://doi.org/10.1109/TIE.2021.3139237.

[32] A. Nurettin and N. İnanç, "Sensorless vector control for induction motor drive at very low and zero speeds based on an adaptive-gain super-twisting sliding mode observer," *IEEE Journal of Emerging and Selected Topics in Power Electronics*, vol. 11, no. 4, pp. 4332-4339, 2023, doi: https://doi.org/10.1109/JESTPE.2023.3265352.

[33] H. Alshatti, "An adaptive soft computing model for flux estimation and torque control of induction motors," *International Journal of Advances in Scientific Research and Engineering*, vol. 10, no. 5, pp. 1-9, 2024, doi: https://doi.org/10.31695/IJASRE.2024.5.1.

TÓM TẮT

PHÂN TÍCH ƯỚC LƯỢNG TỪ THÔNG RÔTO DỰA TRÊN MÔ HÌNH ĐIỆN ÁP CHO CÁC PHƯƠNG PHÁP ĐIỀU KHIỂN VÒNG KÍN KHÔNG CẢM BIẾN TỐC ĐỘ

Trần Đình Cương*, Phan Trần Đăng Khoa

Khoa Điện - Điện tử, Trường Đại học Tôn Đức Thắng, Thành phố Hồ Chí Minh, Việt Nam

*Email: *trandinhcuong@tdtu.edu.vn*

Động cơ không đồng bộ (IM) là thành phần quan trọng trong nhiều hệ truyền động công nghiệp nhờ cấu trúc đơn giản, chi phí thấp và độ tin cậy cao. Tuy nhiên, việc đạt được khả năng điều khiển tốc độ chính xác và bền vững trong các điều kiện tải thay đổi vẫn là một thách thức đáng kể, đặc biệt đối với các hệ truyền động không sử dụng cảm biến tốc độ. Bài báo này nghiên cứu hiệu quả của phương pháp ước tính tốc độ dựa trên Hệ thống thích nghi mô hình tham chiếu (MRAS). Kỹ thuật ước tính tốc độ này được áp dụng cho hai chiến lược điều khiển động cơ không đồng bộ phổ biến: điều khiển vô hướng sử dụng mô hình điện áp (SC-VM) và điều khiển định hướng từ thông sử dụng mô hình điện áp (FOC-VM). Trong cả hai phương pháp, tốc độ rôto và góc từ thông được ước tính trực tiếp từ các tín hiệu điện áp và dòng điện stato đo được, nhờ đó loại bỏ nhu cầu sử dụng cảm biến tốc độ cơ khí. Kết quả mô phỏng dưới nhiều điều kiện vận hành khác nhau cho thấy chiến lược điều khiển không cảm biến dựa trên MRAS mang lại độ chính xác ước tính cao, đáp ứng động tốt và hiệu suất làm việc ổn định của hệ thống, đồng thời giảm chi phí hệ thống và đơn giản hóa cấu trúc bộ truyền động. Phân tích so sánh cũng chỉ ra rằng điều khiển vô hướng phù hợp với các ứng dụng yêu cầu chi phí thấp và cấu trúc hệ thống đơn giản, trong khi điều khiển định hướng từ thông đáp ứng tốt hơn các yêu cầu về hiệu năng động cao và độ chính xác điều khiển lớn. Những kết quả này cung cấp các cơ sở tham khảo quan trọng trong việc lựa chọn chiến lược điều khiển phù hợp cho các ứng dụng truyền động động cơ không đồng bộ trong thực tế.

Từ khóa: Mô hình điện áp, Điều khiển vô hướng, Điều khiển định hướng từ thông, MRAS.